2. The XFEL Principle

A basic description of the FEL process and the photon beam properties is presented. For a detailed description of FEL theory see [1]–[7]. A simplified approach (in German) can be found in [8]. In Chap. 4 specific properties of the TESLA XFELs are discussed.

2.1. FEL vs. Optical Laser

Radiation from a Free Electron Laser (FEL) has much in common with radiation from a conventional optical laser, such as high power, narrow bandwidth and diffraction limited beam propagation. One of the main differences between the two lasers is the gain medium: In a conventional LASER (Light Amplification by Stimulated Emission of Radiation) the amplification comes from the stimulated emission of electrons bound to atoms, either in a crystal, liquid dye or a gas, whereas the amplification medium of the FEL are “free” (unbound) electrons. The free electrons have been stripped from atoms in an electron gun and are then accelerated to relativistic velocities.

While the electrons are propagating through a long, periodic magnetic dipole array – a so called undulator – the interaction with an electromagnetic radiation field leads to an exponential growth of the radiation emitted by the electrons. This amplification of radiation is initiated by an increasingly pronounced longitudinal density modulation of the electron bunch. The initial radiation field can be an external one, e.g. a seed laser, or an “internal” field, i.e. the spontaneous emission of the undulator. In the latter case it is called a SASE (Self Amplified Spontaneous Emission) FEL [9, 10]. Since the electrons in the FEL are not bound to atoms and thus not limited to specific transitions, the wavelength of the FEL is tunable over a wide range depending on accelerator energy and undulator parameters.

For IR, visible and UV FELs, light amplification can be reached in a multi-pass setup, i.e. by using an optical cavity with mirrors on both sides and the electrons passing the undulator as the gain medium in between. With such an arrangement, which – apart from its normally much larger size – exhibits a certain resemblance to optical laser setups, the light from many successive electron bunches is stored and amplified. For VUV and X-ray FELs, mirrors can no longer be applied due to their low reflectivities in normal incidence geometry at these wavelengths and potential mirror deformation/damage due to the high absorbed powers. Since a SASE FEL operates in the high-gain regime, it does not require an optical cavity and it can hence be used to deliver light in the VUV and X-ray regime. In such a "single pass" SASE FEL the full radiation power builds up from spontaneous emission when an electron beam with high phase space density passes a long undulator just once. While FELs in the visible and UV range can also be realized in synchrotron radiation storage rings, there is a consensus that – due to the higher demands on the electron beam properties –

one needs a linear accelerator to generate FEL radiation in the VUV and X-ray range. The most promising approach is the setup of a single pass SASE FEL at a state of the art linear accelerator in combination with a high-performance radio frequency photo-cathode electron gun and longitudinal bunch compression to achieve the required peak current of several kA. Details on the parameters of such an electron gun, the linear accelerator, bunch compressors, etc. can be found in Part II of this report, describing the machine setup for the TESLA project.

2.2. From Synchrotron Radiation to a SASE FEL

The basic principle of the free electron laser can be described within the standard picture for the generation of synchrotron radiation: while travelling with relativistic velocity ($v \simeq c$, $\gamma \simeq 10^2 - 10^5$) through the undulator, the electrons are accelerated in the direction transverse to their propagation due to the Lorentz force introduced by the magnetic field. They propagate along a sinusoidal path and emit SR in a narrow cone in the forward direction. The typical opening angle of the wavelength integrated radiation is

$$\frac{1}{\gamma} = \frac{m_e c^2}{E_e} \,, \tag{2.2.1}$$

where m_e is the electron mass (511 keV/c^2) and E_e the electron energy. In the undulator, the deflection of the electrons from the forward direction is comparable to the opening angle of the synchrotron radiation cone. Thus the radiation generated by the electrons while travelling along the individual magnetic periods overlaps. This interference effect is reflected in the formula for the wavelength λ_{ph} of the first harmonic of the spontaneous, on-axis undulator emission

$$\lambda_{ph} = \frac{\lambda_u}{2\gamma^2}(1 + K_{rms}^2) \,, \tag{2.2.2}$$

where λ_u is the length of the magnetic period of the undulator and K_{rms} is the "averaged" undulator parameter[1]

$$K_{rms} = \frac{e\, B_u\, \lambda_u}{2\,\pi\, m_e c} \tag{2.2.3}$$

which gives the ratio between the average deflection angle of the electrons and the typical opening cone of the synchrotron radiation. B_u is the rms magnetic field of the undulator and e the electron charge.

The interference condition basically means that, while travelling along one period of the undulator, the electrons slip by one radiation wavelength with respect to the (faster) electromagnetic field. This is one of the prerequisites for the SASE process of the FEL. To obtain an exponential amplification of the spontaneous emission present in any undulator, some additional criteria have to be met: One has to guarantee a good electron beam quality and a sufficient overlap between radiation pulse and electron bunch along the undulator. To

[1] Please note that for a planar undulator and a sinusoidal magnetic field, the commonly used undulator parameter K is related to K_{rms} by $K = \sqrt{2} \cdot K_{rms}$ and equation 2.2.3 can be used for K instead of K_{rms} if B_u is replaced by the peak magnetic field B_0.

achieve that, one needs a low emittance, low energy spread electron beam with an extremely high charge density in conjunction with a very precise magnetic field and accurate beam steering through a long undulator.

Oscillating through the undulator, the electron bunch then interacts with its own electromagnetic field created via spontaneous emission. Depending on the relative phase between radiation and electron oscillation, electrons experience either a deceleration or acceleration: Electrons that are in phase with the electromagnetic wave are retarded while the ones with opposite phase gain energy. Through this interaction a longitudinal fine structure, the so called micro-bunching, is established which amplifies the electromagnetic field (Fig. 2.2.1).

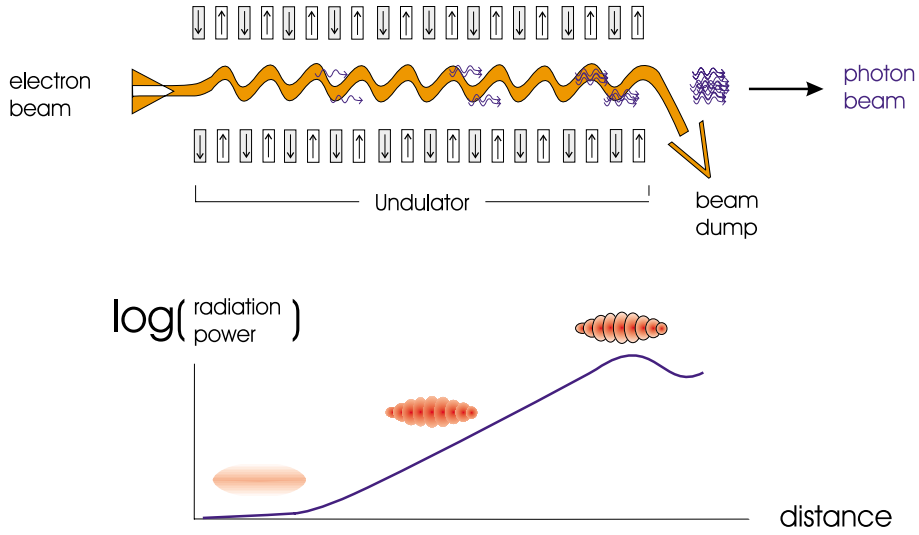

Figure 2.2.1.: *Sketch of the self-amplification of spontaneous emission (SASE) in an undulator resulting from the interaction of the electrons with the synchrotron radiation they emit. In the lower part of the figure the longitudinal density modulation (micro-bunching) of the electron bunch is shown together with the resulting exponential growth of the radiation power along the undulator. Note that in reality the number of micro-bunches is much larger ($\geq 10^{5}$ for the TESLA XFELs).*

The longitudinal distribution of electrons in the bunch is "cut" into equidistant slices with a separation corresponding to the wavelength λ_{ph} of the emitted radiation which causes the modulation. More and more electrons begin to radiate in phase, which results in an increasingly coherent superposition of the radiation emitted from the micro-bunched electrons. The more intense the electromagnetic field gets, the more pronounced the longitudinal density modulation of the electron bunch and vice versa.

In the beginning – without micro-bunching – all the N_e electrons in a bunch ($N_e \geq 10^9$) can be treated as individually radiating charges with the power of the spontaneous emission $\propto N_e$. With complete micro-bunching, all electrons radiate almost in phase. This leads to a radiation power $\propto {N_e}^2$ and thus an amplification of many orders of magnitude with respect

to the spontaneous emission of the undulator.

Due to the progressing micro-bunching, the radiation power $P(z)$ of such a SASE FEL grows exponentially with the distance z along the undulator [1, 11, 12]:

$$P(z) = AP_{in}\exp(2z/L_g) \tag{2.2.4}$$

where L_g is the field gain length, P_{in} the "effective" input power, and A the input coupling factor. A is equal to 1/9 in one-dimensional FEL theory with an ideal electron beam. For the estimation of the effective input power of the shot noise P_{in} one can use the spontaneous radiation power on the first gain length inside a coherence angle and within the FEL bandwidth. The exponential growth takes place until the electron beam is completely bunched (see Fig. 2.2.2) after which it is overmodulated resulting in saturation.

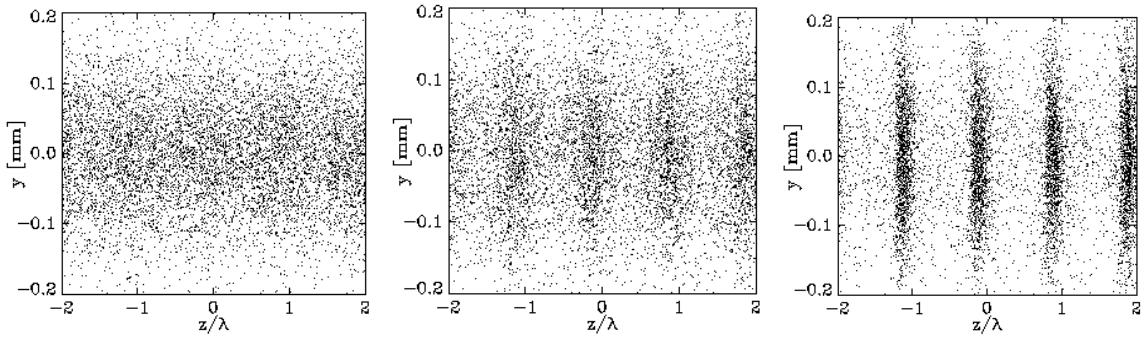

Figure 2.2.2.: *Example of the development of micro-bunching of the XFEL electron beam along the undulator. The electron density is represented by the density of the dots (Left: at the undulator entrance, Middle: in the middle of the exponential growth regime, Right: at the undulator exit, i.e. for saturation). Note that only an enlarged section of the bunch is shown. In reality the number of slices (micro-bunches) is much larger.*

The main properties of the FEL radiation can be simply estimated in terms of the FEL parameter ρ [10]: the field gain length is $L_g \simeq \lambda_u/(4\pi\rho)$, the FEL amplifier bandwidth $\Delta\omega/\omega$ and saturation efficiency (ratio of the output radiation power to the electron beam power) are about ρ. This parameter depends on the parameters of electron beam and undulator and is always much smaller than unity (for the TESLA XFELs ρ ranges between 10^{-3} and 10^{-4}).

The radiation from an X-ray FEL has a narrow bandwidth, it is fully polarized and transversely coherent. The transverse coherence is also reflected in the development of the transverse intensity distribution along the undulator (Fig. 2.2.3) which in the end is nearly Fourier transform limited [1, 13].

On the other hand, compared to conventional optical lasers the longitudinal coherence of an X-ray SASE FEL is rather poor which is a consequence of the start-up from shot noise (see Fig. 2.2.4). The coherence time is defined by the inverse spectral width $\Delta\omega$ and is for XFELs typically much smaller than the electron pulse duration. To improve the longitudinal

coherence length, at best up to the full radiation pulse length, a so called "two-stage SASE FEL" is proposed (see [14] and Chap. 4.2.2), where the final output radiation bandwidth is close to the limit given by the finite duration of the pulse.

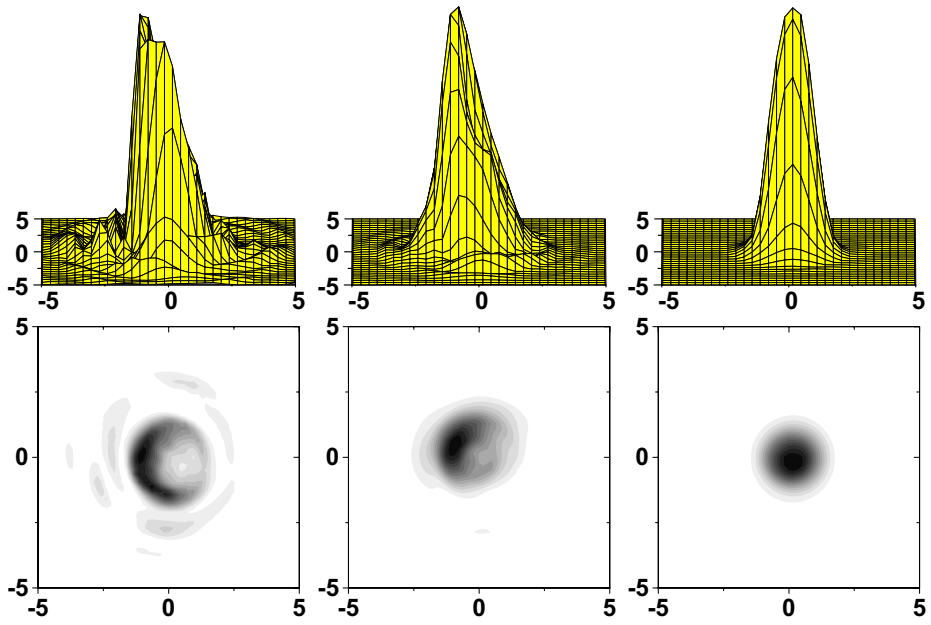

Figure 2.2.3.: *Distribution of the radiation intensity across one slice of the pulse close to the undulator entrance (left), half way through the undulator (middle) and close to saturation (right). The upper figures display the intensity vs. the transverse coordinates, in the lower figures the corresponding polar distribution is shown in units normalized to the radial pulse width* σ_R.

Figure 2.2.4.: *Example of the buildup of coherence along the undulator. The left figure shows the radiation intensity profile half way through the undulator, the figure to the right close to saturation. Please note that for a better visualization of the effect the figures were obtained from a simulation that was made at longer wavelengths and for a coherence length* L_c *which is 10% of the electron bunch length* L_b*, whereas for XFELs the typical ratio is* $L_c/L_b \simeq 10^{-3}$.

Examples of temporal and spectral structure of the radiation pulse from an X-ray FEL are presented in Fig. 2.2.5. The radiation pulse consists of a large number of independent wavepackets which give rise to "spikes". Within one wavepacket, the radiation is transversely and longitudinally coherent. The chaotic nature of the output radiation is a consequence of the start-up from shot noise: since the electron bunch consists of discrete charges randomly emitted from a cathode, the charge density exhibits fluctuations which are random in time and space. As a result, the radiation produced by such a beam has random amplitudes and phases in time and space. These kinds of radiation fields can be described in terms of statistical optics with, e.g., the following parameters: time and spectral correlation functions, transverse correlation functions, probability density distributions of the instantaneous radiation intensity, of its integrals (finite-time and space) and of the energy after a monochromator, coherence time, interval of spectral coherence, coherence area and coherence volume [1].

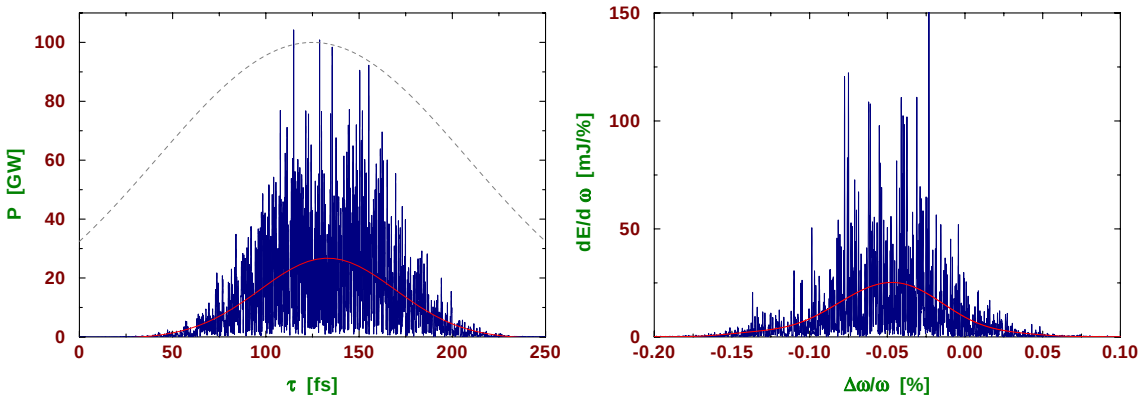

Figure 2.2.5.: *Typical temporal (left) and spectral (right) structure of the radiation pulse from a SASE XFEL at a wavelength of 1 Å. The red lines correspond to averaged values. The dashed line represents the axial density profile of the electron bunch. Note that the growth rate in the electron bunch tail is reduced due to the reduced current. Therefore, the radiation pulse length of 100 fs (FWHM) is about a factor of two shorter than the electron bunch.*

Using a planar undulator, a SASE FEL also naturally generates higher harmonics, since the micro-bunching of the electrons at the fundamental wavelength of the undulator can also drive substantial bunching at the higher harmonics[1]. Simulations yield a significant power output of a high-gain SASE FEL which for the third harmonic amounts to several per thousand up to one percent of the first harmonic output power [15, 16]. Whereas this nonlinear generation of higher harmonics might be quite relevant when extending the FEL operation range to even shorter wavelengths, all quantitative examples in the scientific case

[1] This generation of higher harmonics should not be confused with the so called high gain harmonic generation (HGHG) for FELs. Whereas the mechanism is identical, the HGHG consists of an undulator setup creating a micro-bunching at the first harmonic and a second undulator optimized for a higher harmonic which uses the density-modulated bunch to drive the modulation at this higher harmonic.

and the following chapters are based on the first harmonic of the XFELs.

2.3. Spectral Characteristics

As already mentioned, the characteristics of FEL radiation are high power, short pulse length, narrow bandwidth, spatial coherence and wavelength tunability. In this section, some examples will be given that shed light on the differences between the TESLA XFELs and state-of-the-art synchrotron radiation sources to illustrate the exceptional properties of an FEL. Table 2.3.1 gives an example of some typical photon beam parameters for one of the planned XFELs at TESLA (a detailed discussion of the properties of all XFEL undulators at TESLA can be found in Chap. 4).

	Units	SASE 1
Wavelength*	Å	1–5
Peak power	GW	37
Average power	W	210
Photon beam size (FWHM)**	μm	100
Photon beam divergence (FWHM)***	μrad	0.8
Bandwidth (FWHM)	%	0.08
Coherence time	fs	0.3
Pulse duration (FWHM)	fs	100
Min. pulse separation****	ns	93
Max. number of pulses per train****	#	11500
Repetition rate****	Hz	5
Number of photons per pulse	#	1.8×10^{12}
Average flux of photons	#/sec	1.0×10^{17}
Peak brilliance	B*****	8.7×10^{33}
Average brilliance	B*****	4.9×10^{25}

*Parameters are given for the shortest wavelength.

** Value at the exit of the undulator.

*** Far field divergence.

**** Values determined by the time structure of the electron beam in the accelerator. The average parameters for the SASE-1 FEL are given for the ultimate case when only this beamline is in operation.

***** In units of photons/(sec $\cdot$ mrad^2 $\cdot$ mm^2 $\cdot$ 0.1 % bandwidth).

Table 2.3.1.: *Photon beam properties of the SASE 1 FEL at TESLA. In Chap. 4 photon beam parameters for all FEL devices and also the undulator parameters are presented.*

One of the key parameters to compare different radiation sources is their brilliance[1]. For partially coherent light sources (wigglers and undulators) the brilliance [photons/(sec $\cdot$ mrad^2 $\cdot$ mm^2 $\cdot$ 0.1 % bandwidth)] can be calculated from the spectral flux [photons/(sec $\cdot$

[1]Note: In the US the European "brilliance" is mostly called "brightness".

$0.1\,\%$ bandwidth)] divided by the photon beam's rms radius $\sum$ and divergence $\sum'$ obtained from convolution of the electron beam and photon diffraction parameters as

$$\text{brilliance} = \frac{\text{spectral flux}}{4\pi^2 \cdot \sum_x \cdot \sum'_x \cdot \sum_z \cdot \sum'_z} \tag{2.3.1}$$

$$\text{with} \quad \sum = \sqrt{\sigma_e^2 + \sigma_{ph}^2} \tag{2.3.2}$$

$$\text{and} \quad \sum' = \sqrt{\sigma'^2_e + \sigma'^2_{ph}} \tag{2.3.3}$$

In the case of full transverse coherence (e.g. FELs in saturation) $\sum$ and $\sum'$ are related through

$$\sum\sum' = \frac{\lambda_{ph}}{4\pi} \tag{2.3.4}$$

and Equation 2.3.1 can be transformed into

$$\text{brilliance} = \frac{\text{spectral flux}}{(\lambda_{ph}/2)^2} \tag{2.3.5}$$

This means that the brilliance is simply given by the spectral flux divided by the transverse photon phase space.

As depicted in Fig. 2.3.1 the peak brilliance of the TESLA XFELs surpasses the spontaneous undulator radiation from today's state-of-the-art synchrotron radiation facilities by about eight or more orders of magnitude while the average brilliance is about four orders of magnitude higher (Figure 2.3.2). The peak brilliance is the brilliance scaled to the length of a single pulse while average brilliance is normalized to seconds at the highest possible repetition rate. Figure 2.3.3 shows the number of photons per mode, which can be expressed as

$$\text{No. of Photons/Mode} = \text{Peak Brilliance} \cdot \frac{\lambda_{ph}^3}{4\,c}\ . \tag{2.3.6}$$

Eight orders of magnitude more photons per mode reflect the improved coherence of the FELs compared to the spontaneous emission of third generation SR sources. In summary, extremely short pulses, high intensity and full transverse coherence are the attractive features of the XFEL radiation.

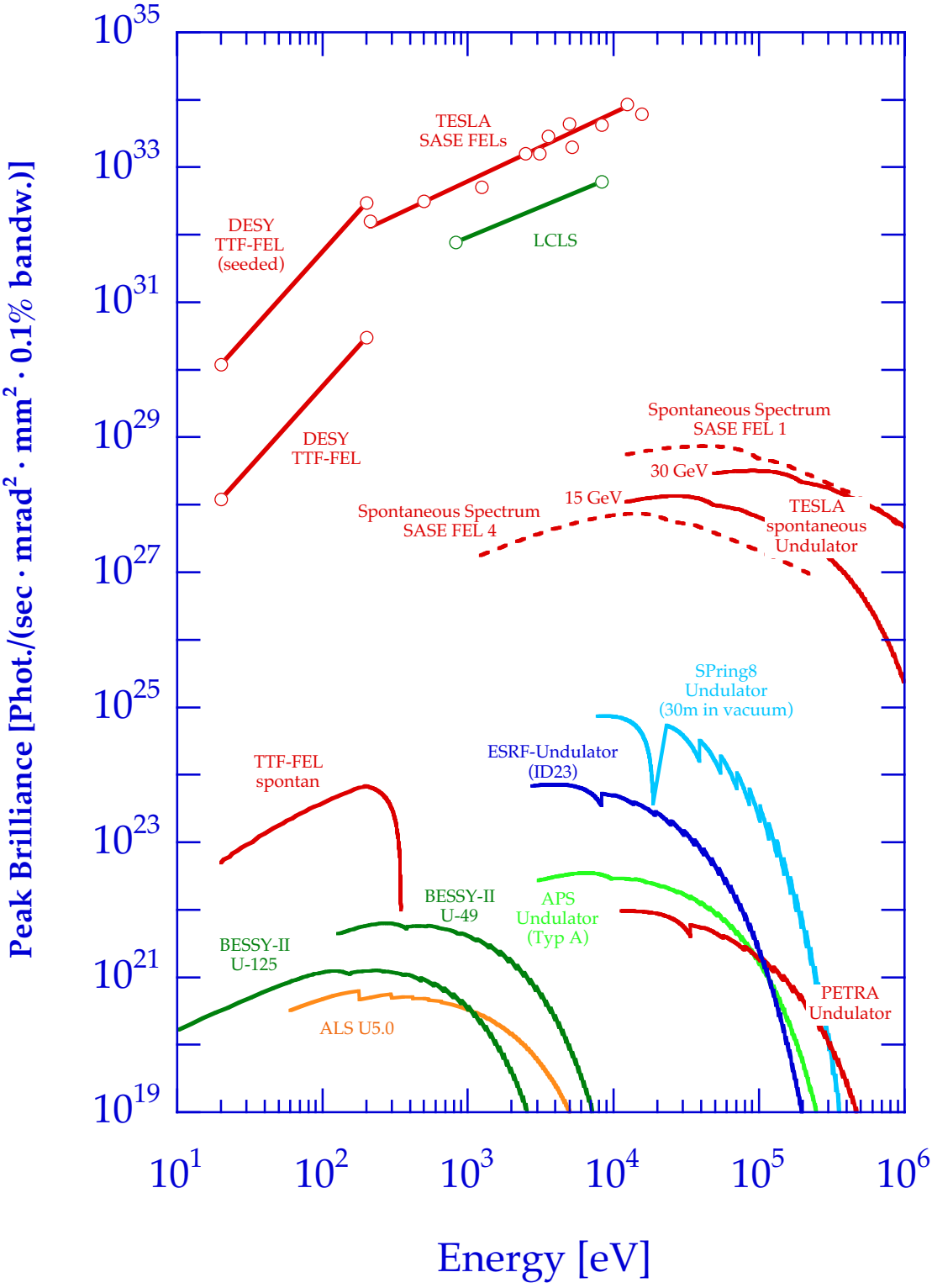

Figure 2.3.1.: *Peak brilliance of XFELs and undulators for spontaneous radiation at TESLA and at the LCLS, Stanford [17], in comparison to the undulators at present third generation synchrotron radiation sources. In addition, also the spontaneous spectrum of an XFEL undulator is shown.*

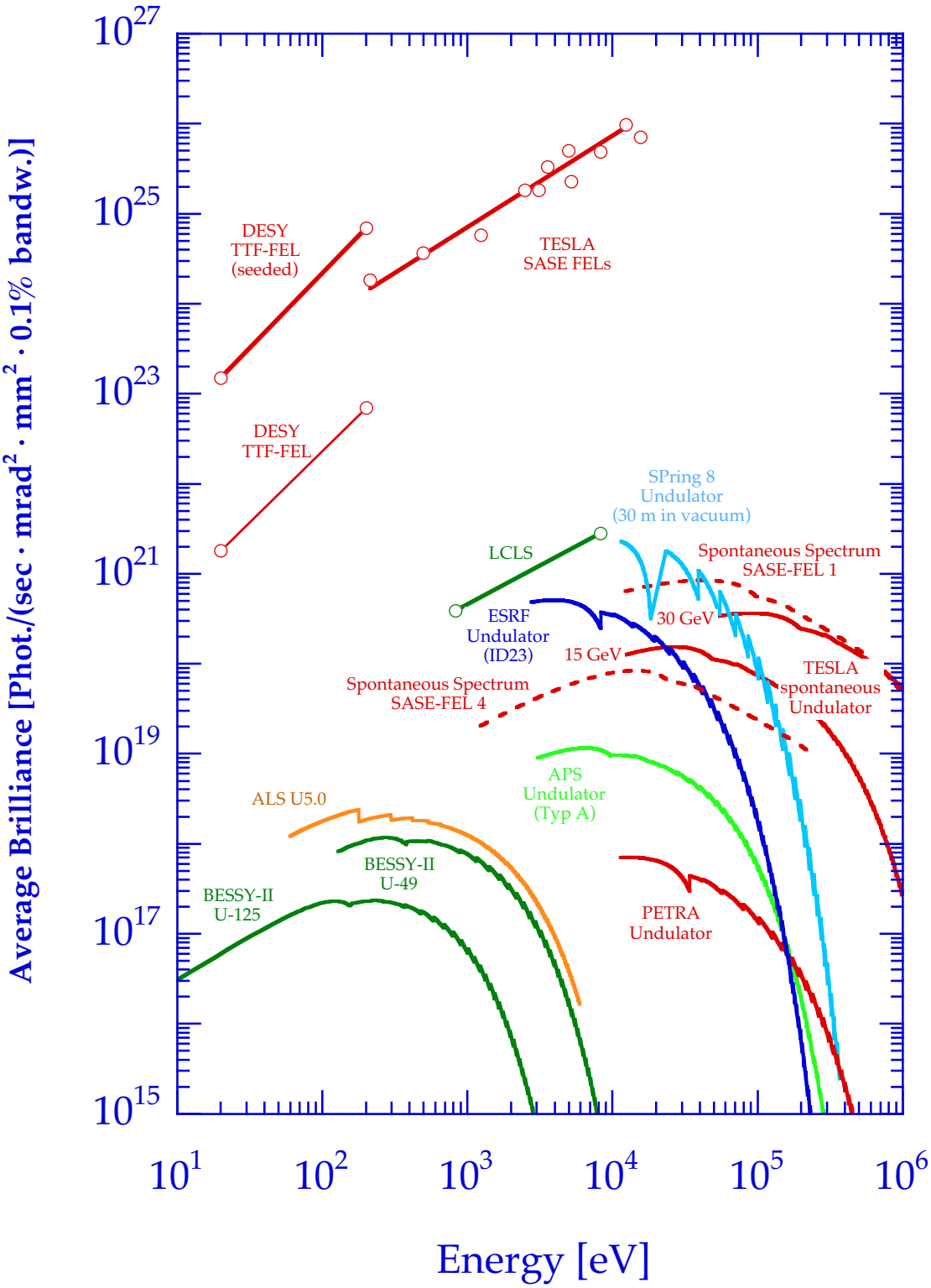

Figure 2.3.2.: *Average brilliance of XFELs and undulators for spontaneous radiation at TESLA and at the LCLS, Stanford [17], in comparison to the undulators at present third generation synchrotron radiation sources. In addition, also the spontaneous spectrum of an XFEL undulator is shown.*

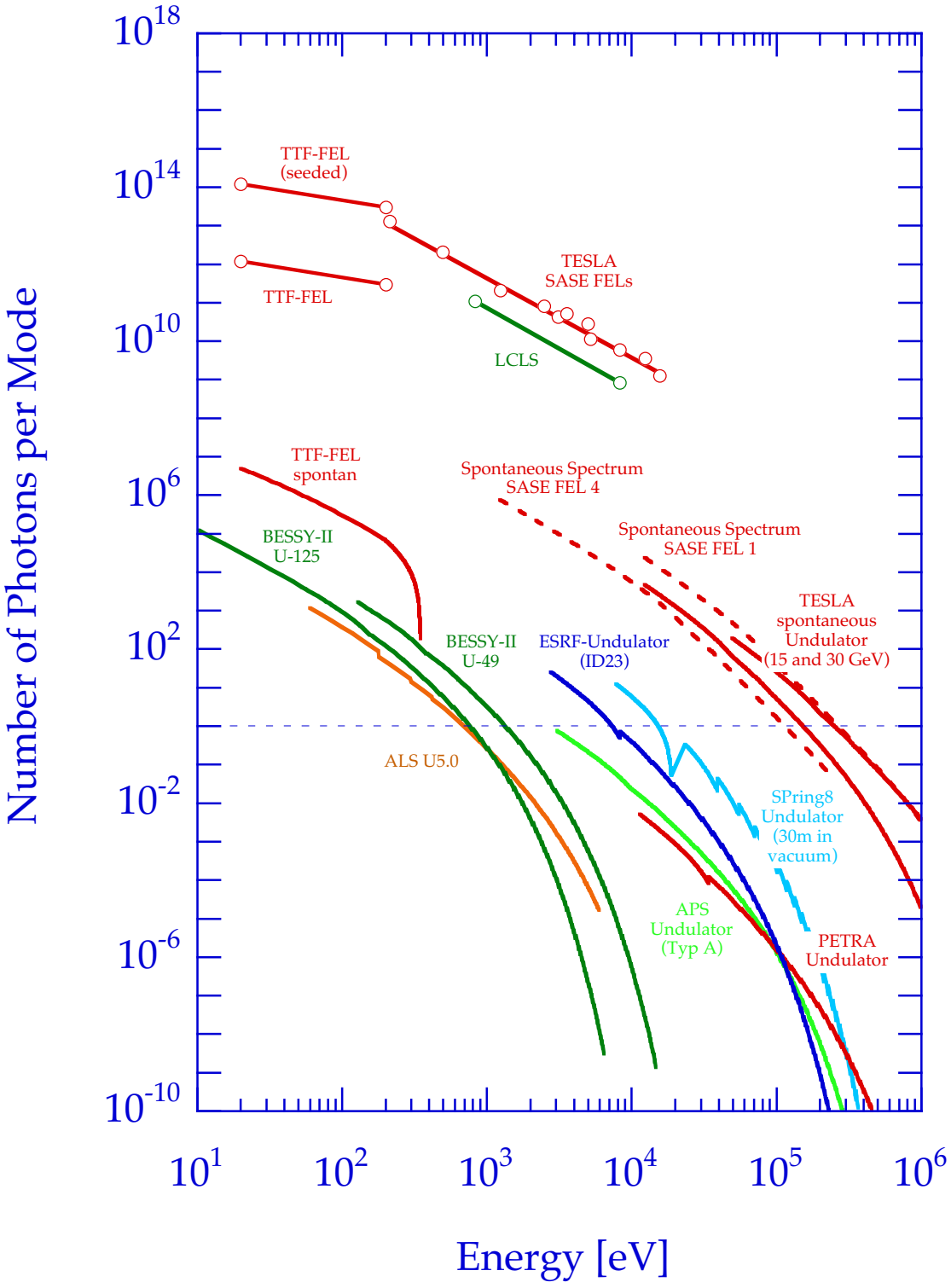

Figure 2.3.3.: *Number of photons per mode for the XFELs and undulators for spontaneous radiation at TESLA and at the LCLS, Stanford [17], in comparison to the undulators at present third generation synchrotron radiation sources. In addition, also the spontaneous spectrum of an XFEL undulator is shown. Please note that these curves were derived using Equation 2.3.6 with a peak brilliance scaled to a bandwidth* $\Delta\lambda/\lambda = 1$.

Bibliography

[1] E.L. Saldin, E.A. Schneidmiller, M.V. Yurkov, *The Physics of Free Electron Lasers*, Springer, Berlin-Heidelberg (2000) and references therein.

[2] T.C. Marshall, *Free Electron Lasers*, MacMillan, New York, NY (1985)

[3] P. Luchini and H. Motz, *Undulators and Free-Electron Lasers*, Oxford Science publications, Oxford (1990)

[4] H.P. Freund and T.M. Antonsen Jr., *Principles of free-electron lasers*, Chapman and Hall, London, UK (1996)

[5] A. Yariv, *Quantum Electronics* (3rd edition), J. Wiley & Sons, New York (1989)

[6] G. Dattoli, A. Renieri, and A. Torre (eds.), *Lectures on the Free Electron Laser Theory and Related Topics*, World Scientific, London (1993)

[7] W.B. Colson, C. Pellegrini, and A. Renieri (eds.), *Laser Handbook*, Vol. 6, North-Holland, Amsterdam (1990)

[8] J. Feldhaus, J. Roßbach und H. Weise, Spektrum der Wissenschaft, Dossier 2/1998: *Laser in neuen Anwendungen*, 106 (1998)

[9] A.M. Kondratenko and E.L. Saldin, Part. Accelerators **10**, 207 (1980).

[10] R. Bonifacio, C. Pellegrini and L.M. Narducci, Opt. Commun. **50**, 373 (1984).

[11] K.J. Kim, Phys. Rev. Lett. **57**, 1871 (1986).

[12] S. Krinsky and L.H. Yu, Phys. Rev. A **35**, 3406 (1987).

[13] E.L. Saldin, E.A. Schneidmiller, M.V. Yurkov, Opt. Commun., in press.

[14] J. Feldhaus, E.L. Saldin, J.R. Schneider, E.A. Schneidmiller and M.V. Yurkov, Opt. Commun. **140**, 341 (1997).

[15] H.P. Freund, S.G. Biedron and S.V. Milton, Nucl. Instrum. and Meth. A **445**, 53 (2000)

[16] Z. Huang and K.-J. Kim, Phys. Rev. E **62**, 7295 (2000)

[17] Values taken from
http://www-ssrl.slac.stanford.edu/lcls/lcls_parms.html